ADVANCED FUNCTIONAL MATERIALS
www.afm-journal.de

Demonstration of an All-Optical AND Gate Mediated by Photochromic Molecules

*Heyou Zhang, Max Gießübel, Pankaj Dharpure, Andrea Albert, Vira Niestierkina, Paul Mulvaney, Mukundan Thelakkat, and Jürgen Köhler**

The realization of a photonic logic AND gate, i.e. a logic AND gate that runs on photons rather than electrons, and where all steps are controlled by light, is demonstrated. In a proof-of-principle experiment, this is accomplished by exploiting photochromic molecules for monitoring the presence or absence of photons of particular wavelengths that represent the logic variables.

1. Introduction

Photochromic molecules change their isomeric state upon illumination with light of suitable wavelengths, thereby offering a simple and contactless method for modulating their photophysical properties by external stimuli.[1–4] Such molecules have been used for photocontrol of biological functions, bioimaging, super-resolution fluorescence microscopy, fluorescence color modulation, demonstration of an optical transistor, targeted pharmacology, control of chemical reactivity, or as nanoscale actuators.[5–13] For those types of photochromic molecules, where the chemical bistability is associated with high- and low-emissive states, the two isomers can be considered as photon processing elements, which makes these molecules excellent candidates for the development of all-optical photonic gates and optical memories on the microscale.[2,3,14–16] Generally, the type of gates can be divided into sequential logic devices, i.e. those where the state of the output depends on the order of the sequence of input signals, and combinational logic gates, i.e. those where the state of the output does not depend on the order of the input signals. Sequential logic gates are appealing and can be used for optical keypad locks because the inputs/outputs act like a PIN code.[17,18] However, the requirement for a defined order of the input signals is in conflict with the commutativity law of Boolean algebra, and therefore only combinational logic gates can be used for logic circuits.

In recent years, perfluorocyclopentene diarylethene (DAEs) photoswitchable molecules have attracted considerable attention owing to their excellent thermal stability and fatigue resistance.[1,2] This has generated a wealth of research and fascinating experiments have been reported that use photochromic molecules for optical data processing.[3,4,19] Simple logic gates as well as sophisticated functionalities including adders, subtractors, encoders, keypad locks etc.[14] have all been realized on the molecular scale. However, in none of these cases were all of the steps purely optical and additional input variables such as chemical transformations or temperature changes were exploited as well. Moreover, most of the experiments relied on solution-based molecular devices, i.e. fluids. Yet, for the realization of all-optical gates it is essential to combine photonic units such that the output of one unit serves as the input of another unit, and this in turn requires the incorporation of the photochromic molecules into solid-state platforms.

Probably the simplest combinational logic gate is the AND gate that connects two inputs with one output. The logical connection between the molecular units is challenging, and photonic concatenation of NAND and AND logic gates has been demonstrated in ref. [20,21] using rare-earth-based nanocrystals. The repetition rate and the pulse widths of the laser excitation source were employed as logic inputs as well as the temperature dependence of the emission. In addition to the DAE molecular building blocks used in the above studies, which alone do not emit in both open and closed forms, there is a new type of photoswitchable molecules, viz., the benzothiophene-perfluorocyclopentene-dioxide (BTCPO4) derivatives of DAEs, which emit strongly in the closed form and which are known as "turn-on" switches (SW).[13,22–24] We make use of 5 different BTCPO4 derivatives

H. Zhang, M. Gießübel, A. Albert, V. Niestierkina, J. Köhler
Spectroscopy of Soft Matter
University of Bayreuth
95440 Bayreuth, Germany
E-mail: juergen.koehler@uni-bayreuth.de
P. Dharpure, M. Thelakkat
Applied Functional Materials
University of Bayreuth
95440 Bayreuth, Germany
P. Mulvaney
ARC Centre of Excellence in Exciton Science
School of Chemistry
University of Melbourne
Parkville, VIC 3010, Australia
M. Thelakkat, J. Köhler
Bavarian Polymer Institute
University of Bayreuth
95440 Bayreuth, Germany
M. Thelakkat, J. Köhler
Bayreuther Institut für Makromolekülforschung (BIMF)
95440 Bayreuth, Germany

The ORCID identification number(s) for the author(s) of this article can be found under https://doi.org/10.1002/adfm.202507180

DOI: 10.1002/adfm.202507180

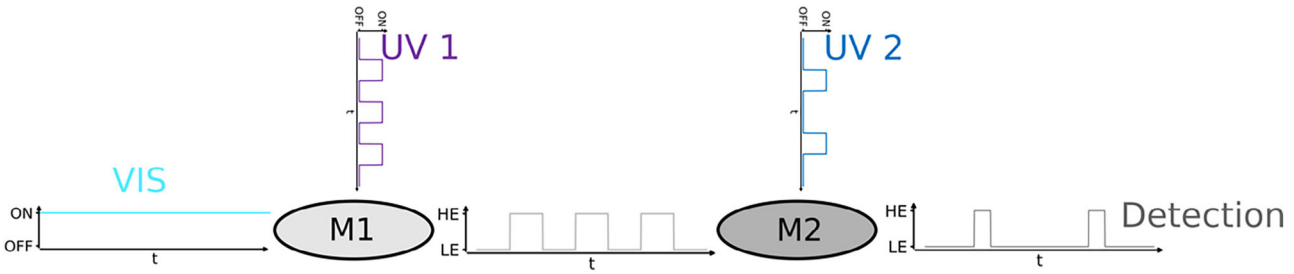

Figure 1. Schematic sketch of two photonic units where the output of the first unit serves as input for the second unit. The ellipses represent photochromic molecules on the optical microscope stages M1 and M2, respectively, that can be converted between HE and LE states upon illumination with light in the UV and VIS spectral ranges (UV1 purple; UV2 blue). Excitation of molecules on M1 to the HE state with visible light (VIS cyan) results in the emission of visible light from these molecules (light grey) which serves as input in the visible spectral range for the molecules on M2. Accordingly, the emission from molecules on M2 will be modulated in intensity as a function of both UV illumination sequences.

(which are labeled SW-1 to SW-5 for simplicity) emitting at different wavelengths for realizing all-optical gates. The synthesis details are given in the experimental section and the supporting information.

Here, as a proof-of-principle, we demonstrate the implementation of an all-optical AND gate, converting two optical inputs into one optical output. The gate depends exclusively on the presence or absence of photons for creating the boolean input and output variables. To achieve this, we cascaded two spatially separated microscopes, referred to as microscope 1 (M1) and microscope 2 (M2) hereafter, and placed two different derivatives of BTCPO4 on each of the microscopes; SW-1 on M1, and molecules of SW-2, SW-3, SW-4, or SW-5 on M2. These molecules all undergo a ring-cyclization reaction upon illumination in the UV, and a ring-opening reaction upon illumination in the VIS spectral range. The isomers are associated with a high-emissive state (HE) in the closed-ring conformation and a low-emissive state (LE) in the open-ring conformation. The idea is to use the emission from the photochromic molecules placed on M1 as input for the photochromic molecules placed on M2, and to study the signal emerging from the molecules on M2 as a function of the status of both types of photochromic switches. This strategy is sketched in **Figure 1**, where the ellipses denote the two types of photochromic molecules on M1 and M2 that can be converted into the HE state upon UV illumination (purple (UV1) for molecules on M1 and blue (UV2) for molecules on M2), and back to the LE state upon illumination in the VIS (cyan for molecules on M1 and light grey for molecules on M2). The molecules on M1 in the HE state can be excited in the visible (cyan), leading to the emission of visible light (light-grey) that is modulated in intensity according to the ON/OFF times of UV1. Using the modulated emission from the molecules on M1 to optically probe the molecules on M2, allows control of the emission from the molecules on M2 as a function of the interplay of the ON/OFF cycling times of both UV sources.

2. Experimental Section

2.1. Synthesis

As photochromic molecules we used 1,2-Bis(2-ethyl-6-phenyl-1-benzothiophene-1,1-dioxide-3-yl)perfluorocyclopentene (SW-1), 1,2-Bis(2-ethyl-6-(thiophen-2-yl)-1-benzothiophen-1,1-dioxide-3-yl)perfluorocyclo-pentene (SW-2), 1,2-Bis(2-ethyl-6-(benzothiophen-2-yl)-1-benzothiophen-1,1-dioxide-3-yl)perfluorocyclopentene (SW-3), 1,2-Bis(2-ethyl-6-(benzothiophen-3-yl)-1-benzothiophen-1,1-dioxide-3-yl)perfluorocyclopentene (SW-4), and 1,2-Bis(2-ethyl-6-(napthalen-2-yl)-1-benzothiophen-1,1-dioxide-3-yl) perfluorocyclopentene (SW-5). See Supporting Information for details of the synthetic procedures and characterization of the BTCPO4 molecules.

2.2. Sample Preparation

All dyes were dissolved in toluene at a mass concentration of 0.135 mg mL^{-1} corresponding to the following molar concentrations: SW-1: 0.188 mM, SW-2: 0.186 mM, SW-3: 0.164 mM, SW-4: 0.164 mM, SW-5: 0.166 mM. This stock solution was mixed with 5% PMMA in toluene in a 1:1 ratio and stirred for 10 min. A small amount of the mixture (100 µL) was drop cast on a quartz cover slide and spin-coated at 1000 rpm for 150 s.

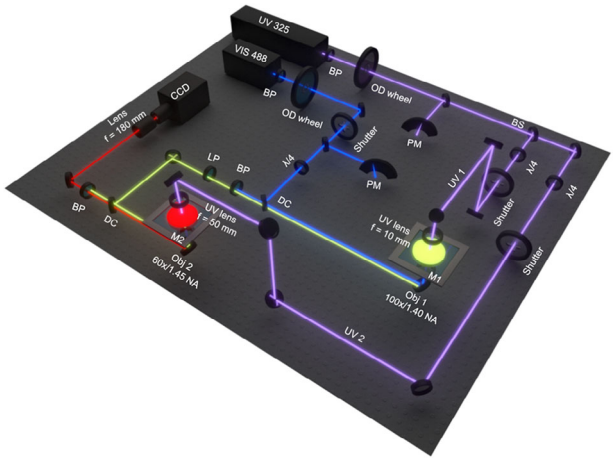

Figure 2. Schematic sketch of the two-microscope setup. The light sources are indicated as UV (325 nm) and VIS (488 nm). The two microscopes are referred to as M1 and M2. The abbreviations denote: BP - bandpass filter, LP - long pass filter, BS - beam splitter, DC - dichroic mirror, OD - optical density, PM - power meter, $\lambda/4$ - quarter waveplate, CCD - charge-coupled device.

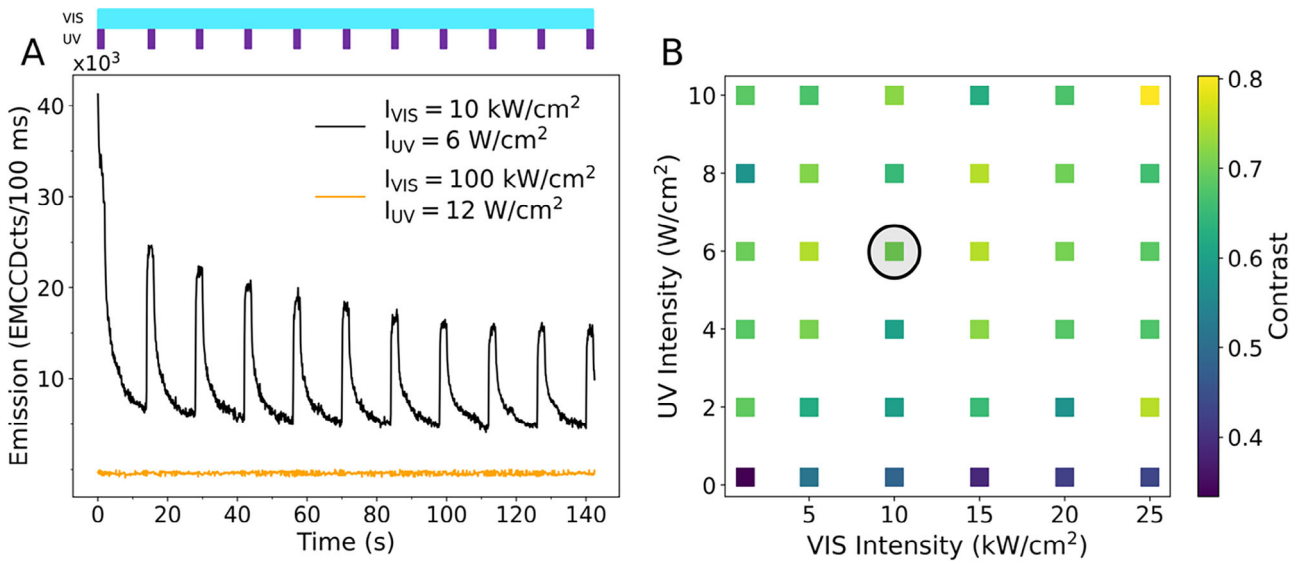

Figure 3. A) The black line shows the emission intensity from the pyridine molecules on M2 as a function of the illumination conditions of SW-1 on M1. The sample on M1 was illuminated for 2 s at 325 nm with 6 W cm^{-2} followed by an off period of 12 s. The VIS illumination at 488 nm with 10 kW cm^{-2} was continuous. This illumination sequence is indicated by the colored bars at the top. The yellow line shows the result of a reference experiment with a bare glass substrate on M2 using the same illumination sequence, yet intensities of 12 W cm^{-2}, and 100 kW cm^{-2}, for the UV and VIS lasers, respectively. B) Achievable contrast, for the modulation of the emission intensity of the pyridine sample as a function of the UV and VIS illumination intensities. The horizontal axis corresponds to the VIS intensity, the vertical axis to the UV intensity, and the achieved contrasts are given by the color code. The marked dot corresponds to the experiment shown in part A) of the figure.

2.3. Optical Setup

The optical setup comprises two, spatially separated, home-built microscopes, M1 and M2, that are cascaded so they operate in tandem, **Figure 2**.

Visible light (VIS) at 488 nm (blue line) is provided by a laser diode (PC13781, 40 mW, Spectra-Physics). It passes a bandpass filter (BP 488/10, AHF) for clean-up and a variable OD tuning wheel (OD 0.04-3.0, Edmund Optics) for adjusting the output power. The intensity behind the OD wheel is monitored by a powermeter (PM100A, Thorlabs). The light is converted to circular polarization by a quarter waveplate (200–1600 nm, New Focus) in order to avoid photoselection, then reflected by a dichroic beam splitter (reflection 350–458 nm > 90%, transmission 464–900 nm > 93%, AHF), and focussed onto the sample on M1 with an objective (100x, NA 1.40 UPlanSApo oil objective, Olympus). For both microscopes a helium-cadmium laser (He-Cd, IK3201R-F, Kimmon) served as light source for the UV radiation at 325 nm (purple line). Its output passes a bandpass filter (BP 320/40, AHF), and a variable OD tuning wheel (OD 0.04-4.0, Edmund Optics) for clean-up and adjustment of the intensity which was also monitored by a powermeter (FieldMax II, Coherent). The UV light was split by a 50:50 beam splitter (BSW20 Ø1, Thorlabs), and each of the two resulting beams was directed to one of the microscopes M1 and M2, referred to as UV1 and UV2 hereafter. In order to avoid photoselection the UV1 light was converted to circular polarization using a quarter waveplate (260–410 nm, Thorlabs) and focussed with a lens (Quartz, f = 10 mm, Edmund Optics) onto the sample on M1 such that the foci of the VIS and UV1 radiation coincided. The emission from the sample on M1 (green line) is collected by the same objective and passes the dichroic mirror, a bandpass filter (BP 578/105, AHF), and a longpass filter (LP 488, AHF) to suppress residual laser light. Then it is reflected by another dichroic mirror (reflection 420–610 nm > 95%, transmission 635–950 nm > 90%, AHF) and focussed onto the sample on M2 with an objective (60x, NA 1.45 PlanApo oil objective, Olympus). The UV2 radiation is also converted to circular polarization (260–410 nm, Thorlabs), and focussed with a lens (Quartz, f = 50 mm, Edmund Optics) onto the sample on M2 such that the foci of the emission collected from M1 and the UV2 radiation coincided. The ON/OFF switching of all three laser beams, VIS, UV1, and UV2 was controlled independently with mechanical shutters (VIS/UV 1: LS6 6 mm, Uniblitz; UV2: home-built). The signal emitted from the molecules on M2 (red line) is collected by the M2 objective and transmitted through the second dichroic and a bandpass filter (BP 660/52, AHF). Finally, the signal is focussed with a tube lens (f = 180 mm, U-TLUIR, Olympus) onto a charge-coupled device (CCD camera, iXon, DV887, 2006, Andor) and read out with a bin time of 200 ms.

3. Results and Discussion

We started by placing a sample with photochromic molecules on M1 and a sample with dye molecules on M2. For this purpose SW-1 was chosen for the photochromic sample, and pyridine 2 (4-[4-[4-(Dimethylamino)phenyl]-1,3-butadienyl]-1-ethylpyridinperchlorate) for the dye, because its absorption spectrum exhibits good overlap with the emission spectrum of the photochromic molecules (see Supporting Information). Under typical excitation conditions an order of magnitude estimate of the number of photons that can be transferred from M1 to M2 yields 2.5 · 10^6 s^{-1} per SW-1 molecule (see Supporting Information), which is sufficient for acting as excitation source for the dye molecules on M2.

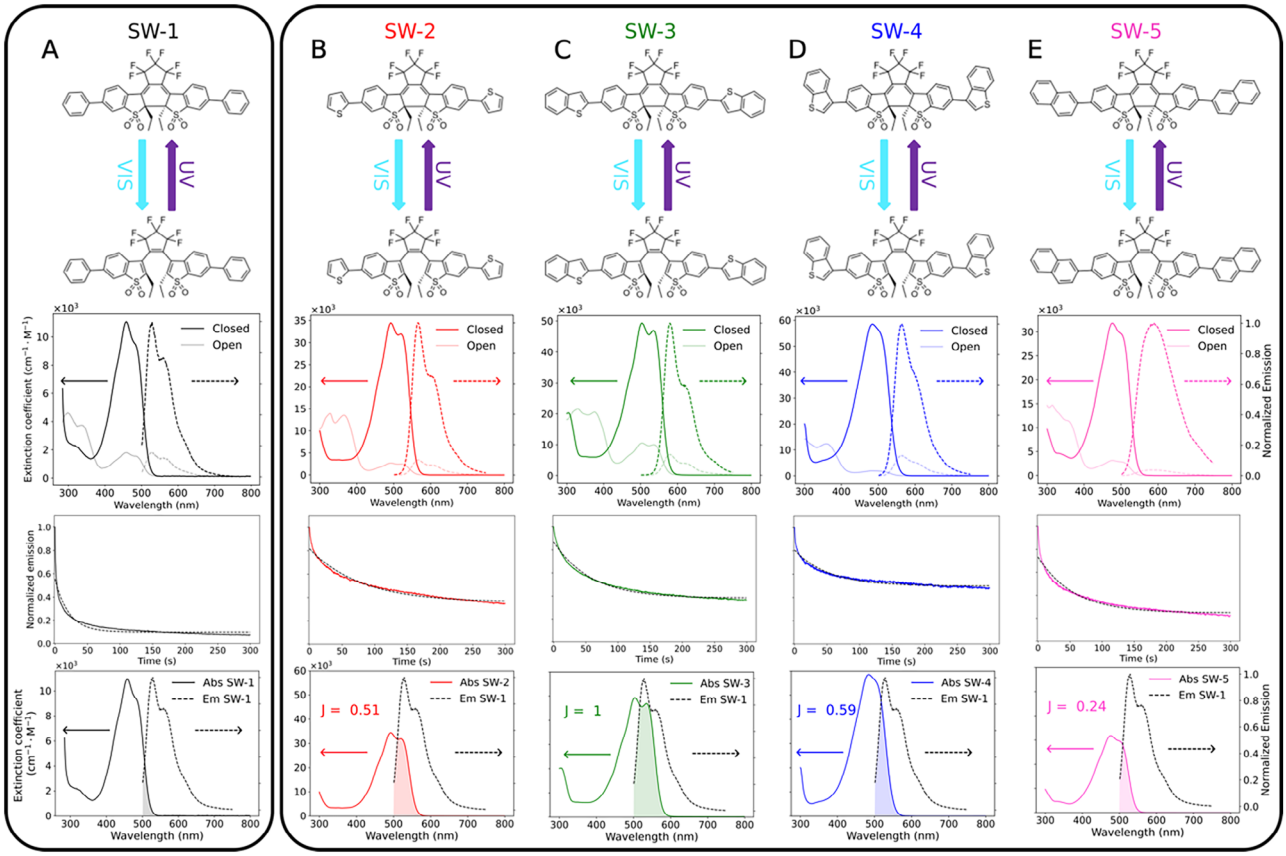

Figure 4. Columns A–E) refer to the different types of photochromic molecules. Each panel shows from top to bottom the structures of the molecules in the closed (HE) and open (LE) conformation, the absorption and emission spectra in toluene at 21°C for the two conformations, the relative decrease of the emission intensity of the HE state upon VIS illumination (colored lines) together with a fit (black dashed lines), and the spectral overlap, *J*, (shaded area), of the normalized emission spectrum from SW-1 (black dotted line) with the absorption spectra of SW-2, SW-3, SW-4, and SW-5 (colored lines), respectively. For ease of comparison the overlaps are normalized relative to the one between SW-1 and SW-3. To record the emission from the HE state (third row) the samples were illuminated with UV light for 5 s at 28 W cm^{-2} and VIS light at 430 W cm^{-2} to initialize the molecules in the HE state and subsequently probed with VIS light for 300 s at 430 W cm^{-2}.

The sample on M1 was illuminated continuously with the VIS laser, while the UV laser was switched ON for 2 s followed by an OFF period of 12 s. The modulated emission from the sample on M1 served as excitation light source for the dye molecules on M2 whose emission was registered as a function of the UV and VIS illumination intensities on M1. Indeed, the signal strength of the emission from the dye molecules followed the intensity of the output from the photochromic molecules on M1, **Figure** 3A. For quantitative analysis we defined the normalized contrast as $C = \frac{I_{max} - I_{min}}{I_{max}}$, where I_{max} (I_{min}) refers to the maximum (minimum) of the emission intensity from the pyridine dye, and studied the achievable contrast as a function of the UV and VIS illumination conditions, Figure 3B. In order to make sure that the signal detected did not stem from the emission of the photochromic molecules on M1, or from scattered laser light, the test experiment was repeated with a bare glass substrate on M2 and significantly higher laser intensities. For this control experiment no fluorescence from the dye was observable, Figure 3A yellow line. This testifies that the modulated emission from pyridine reflects the modulation of the output of the photochromic molecules on M1. The test demonstrated that the emission from the photochromic molecules on M1 is strong enough to serve as excitation light source for the dye molecules on M2 and to modulate their emission intensity with a contrast of up to 80%.

The application of this idea to two photochromic molecules requires that the emission from the photoswitches on M1 is absorbed by the photoswitches on M2 in order to induce emission from these molecules. Thus, an essential prerequisite is that the emission spectrum from the photoswitches on M1 features significant spectral overlap with the absorption spectrum of the photoswitches on M2. Therefore, we tested various combinations of photochromic switches. For doing so we used the molecules of SW-1 on M1, and molecules of SW-2, SW-3, SW-4, SW-5 on M2. The structure of all photochromic molecules used in this study in both isomeric states is shown at the top of **Figure** 4. Furthermore Figure 4 shows from top to bottom the corresponding absorption and emission spectra of the various photochromic molecules in both isomeric states, the recovery of the LE states upon VIS illumination (manifested as a decrease of the emission intensity) together with an exponential fit (for details see

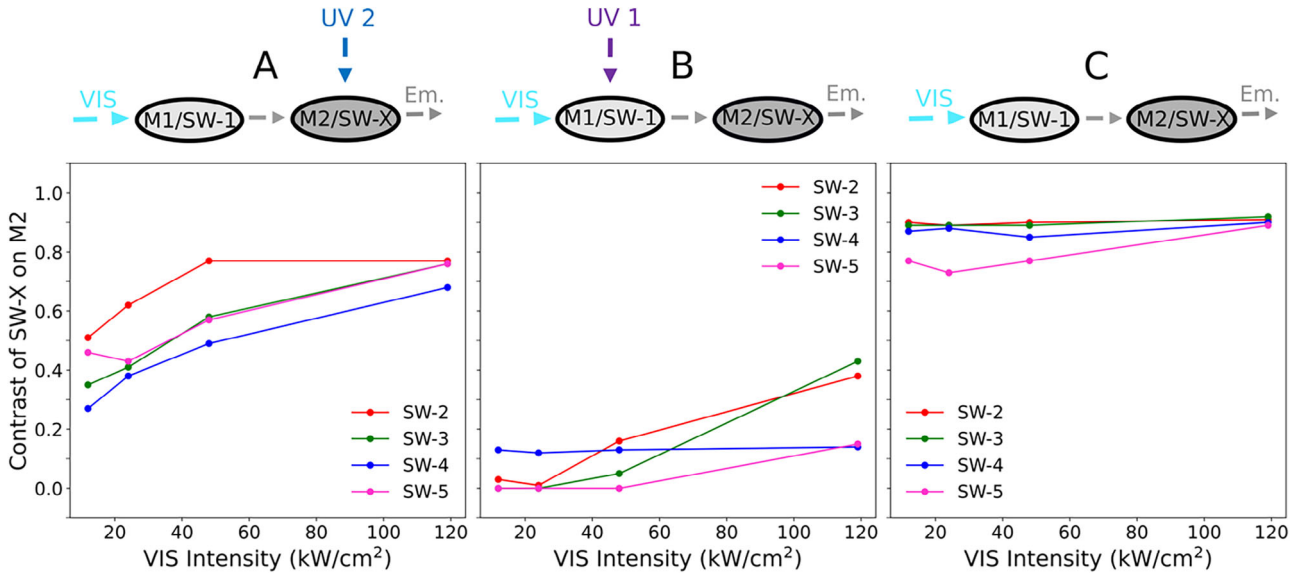

Figure 5. The signal contrast, $C = \frac{I(5s+200\ ms)-I(300\ s)}{I(5s+200\ ms)}$ of the emission from molecules on M2 as a function of the VIS intensity used on M1 for three different illumination scenarios as indicated at the top. For all three scenarios the samples were initialized by illumination for 5 s with UV1 (28 W cm^{-2}), UV2 (0.8 W cm^{-2}), and varying VIS (12, 24, 48, 120 kW cm^{-2}). A) Contrast after continuous illumination for 300 s with varying intensities of visible light (12, 24, 48, 120 kW cm^{-2}) on M1, and UV2 (0.8 W cm^{-2}) on M2. B) Contrast after continuous illumination for 300 s with varying intensities of visible light (12, 24, 48, 120 kW cm^{-2}), and UV1 (28 W cm^{-2}) both on M1. For SW-5 (pink) the contrast is not significantly above the noise floor of the signal for the lowest intensities and has therefore been set to zero. C) Contrast after continuous illumination for 300 s with varying intensities of visible light (12, 24, 48, 120 kW cm^{-2}) on M1 only. The different colors refer to the different photochromic molecules placed on M2, and the lines between the data points serve as a guide for the eye.

Supporting Information), and the spectral overlap, $J = \int F(\lambda)\varepsilon(\lambda)\mathrm{d}\lambda$ between the normalized emission spectrum of SW-1 and the absorption spectra of SW-X (X = 2,3,4,5) (color shaded).

Fitting the recovery of the LE states to an exponential profile allowed us to obtain an estimate for the quantum yield φ_{co} of the ring-opening reaction (for details see the Supporting Information), which amounted to $\approx 10^{-7}$ for all of the diarylethene variants. For the experiments described below, we kept SW-1 as the photochromic molecules on M1 and placed the photochromic molecules SW-X (X = 2, 3, 4, and 5) on M2. The detected signal corresponds always to the emission from the SW-X molecules as a function of time after the initialization. The latter refers to a period of 5 s of illumination with all three light sources, namely VIS and UV1 on M1 and UV2 on M2. Yet, in contrast to the test experiment where the UV source illuminated exclusively the molecules on M1, here the UV light illuminates molecules on both microscopes in order to trigger the open-to-close photoreaction. However, the UV light on M2 gives rise to a weak emission from the SW-X molecules in the open LE state, see Figure 4 2nd row, which has to be taken into account for properly defining the contrast of the signal from the SW-X molecules. Hence, for the contrast $C = \frac{I_{max}-I_{min}}{I_{max}}$ we assign $I_{max} = I(5s + 200\ ms)$, which refers to the emission intensity from SW-X during the first 200 ms time bin after the UV2 illumination has ceased, and $I_{min} = I(300\ s)$ as before to the intensity 300 s after starting the initialization, i.e. $C = \frac{I(5s+200\ ms)-I(300\ s)}{I(5s+200\ ms)}$.The achievable contrasts for the outputs of the SW-X molecules on M2 are shown in **Figure 5** for three different illumination scenarios and for four different VIS intensities.

For the results shown in Figure 5A, the UV1, UV2, and VIS sources were ON for 5 s, followed by a period of 295 s (= 300–5 s) where the samples were illuminated only with VIS and UV2 light. The UV1 and UV2 radiation initializes the photochromic molecules on M1 and M2, SW-1 and SW-X, respectively, into their HE states. The continuous illumination of the SW-1 molecules on M1 with VIS light leads to the emission of photons (fluorescence). Since the SW-X molecules on M2 are kept in the HE state by the continuous illumination with UV2, the emission from SW-1 serves as excitation light for the HE SW-X molecules and gives rise to the emission of photons from these molecules. For all molecules SW-X placed on M2, the contrast of the fluorescence signal grows for higher VIS illumination intensities of SW-1 on M1. For the results shown in Figure 5B the samples were initialized as before for 5 s by illumination from all three light sources. Subsequently, the VIS and UV1 radiation sources were kept ON and the UV2 light was OFF. As before, the excitation of the HE SW-1 molecules in the VIS leads to the emission of photons that triggers the emission from the HE SW-X molecules, and the achievable contrast grows with increasing VIS illumination intensity on M1.

Finally, after the initialization of the samples for 5 s as before, only the VIS radiation was kept ON, Figure 5C. For this scenario the achievable contrast in the emission of the SW-X molecules does not depend significantly on the VIS excitation intensity (and also not much on the type of photochromic molecule placed on M2).

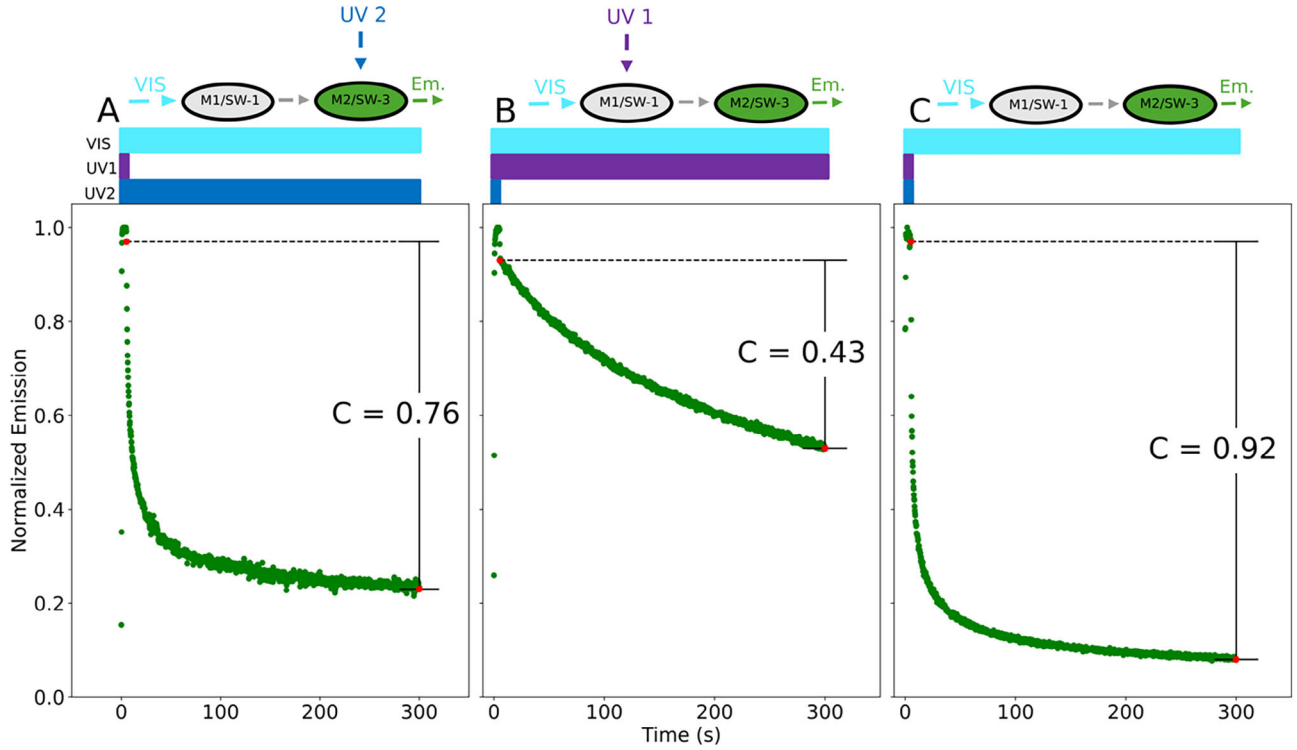

Figure 6. The output of an experiment with SW-1 molecules on M1 and SW-3 molecules on M2 for three different illumination scenarios. The colored bars on top correspond to the illumination times with VIS (cyan), UV1 (purple), and UV2 (blue), i.e. 5 s of initialization by illumination from all three light sources VIS (120 kW cm^{-2}), UV1 (28 W cm^{-2}), and UV2 (0.8 W cm^{-2}), and 295 s illumination with varying illumination conditions as indicated also by the pictograms. The ordinate refers to the respective peak normalized intensity of the emission detected from the SW-3 molecules. UV1 and VIS radiation is applied to the molecules on M1 while UV2 radiation is applied to molecules on M2. The excitation intensities after initialization were A) VIS 120 kW cm^{-2}, UV2 0.8 W cm^{-2}, B) VIS 120 kW cm^{-2}, UV1 28 W cm^{-2}, C) VIS 120 kW cm^{-2}. The values for the signal contrast $C = \frac{I(5s+200\ ms)-I(300\ s)}{I(5s+200\ ms)}$ were obtained between the data points marked in red as explained in the text, and amount to $C = 0.76$, $C = 0.43$, and $C = 0.92$, respectively, as indicated in the figure.

In the following, we will exemplify the demonstration of an optical AND gate using the example of the pair of photochromic molecules SW-1 (on M1) and SW-3 (on M2), because these species feature the largest spectral overlap. The results obtained using SW-1 on M1 and the other BTCPO4 derivatives on M2 will be summarized at the end of this section. The output from the SW-3 molecules on M2 is shown in **Figure 6** for the three different illumination scenarios described above, and as indicated on the top of the figure by the colored bars and the pictograms. For the three scenarios we chose as excitation intensities for the VIS light 120 kW cm^{-2} because this gave the highest contrast in the emission on M2, see Figure 5.

For the results shown in Figure 6A, the UV1, UV2, and VIS sources were ON for 5 s, followed by a period of 295 s where the samples were illuminated only with UV2 and VIS light. The UV1 and UV2 radiation initializes the photochromic molecules SW-1 and SW-3 in the HE states on M1 and M2 microscopes respectively. After the UV1 is turned OFF, the continuous illumination of the SW-1 molecules on M1 with VIS light leads to the emission of photons (fluorescence). Since the SW-3 molecules on M2 are kept in the HE state by the continuous illumination with UV2, the emission from SW-1 serves as excitation light for the HE SW-3 molecules and gives rise to the emission of photons from these molecules. However, on M1 the continuous VIS illumination of the SW-1 molecules can also initiate the ring-opening reaction. Since the open isomer is associated with the LE state the emission from SW-1 fades out, and so does the excitation of the HE SW-3 molecules on M2. This is observable as a decay of the emission from SW-3 during the observation time. The contrast for these illumination conditions read out 300 s after starting the initialization amounts to $C = 0.76$. For the results shown in Figure 6B the samples were initialized as before for 5 s by illumination from all three light sources. Subsequently, the VIS and UV1 radiation sources were kept ON and the UV2 light was OFF. As before the excitation of the HE SW-1 molecules by the VIS light source leads to the emission of photons that triggers the emission from the HE SW-3 molecules. Despite the fact that the continuous UV1 illumination keeps the SW-1 molecules in the HE state, the emission from SW-3 diminishes in the course of time the contrast amounts to $C = 0.43$. This reflects the fact that the photons emitted from SW-1 not only induce emission from the HE state of the SW-3 molecules, but also trigger the ring-opening reaction and the conversion of the SW-3 molecules to the LE state. Finally, after the initialization of the samples for 5 s as before, only the VIS radiation was kept ON, Figure 6C. In this case, the emission from SW-3 decays most rapidly, and we obtain the highest contrast $C = 0.92$. This can be understood as follows: First, there is a decrease in the intensity of light emitted

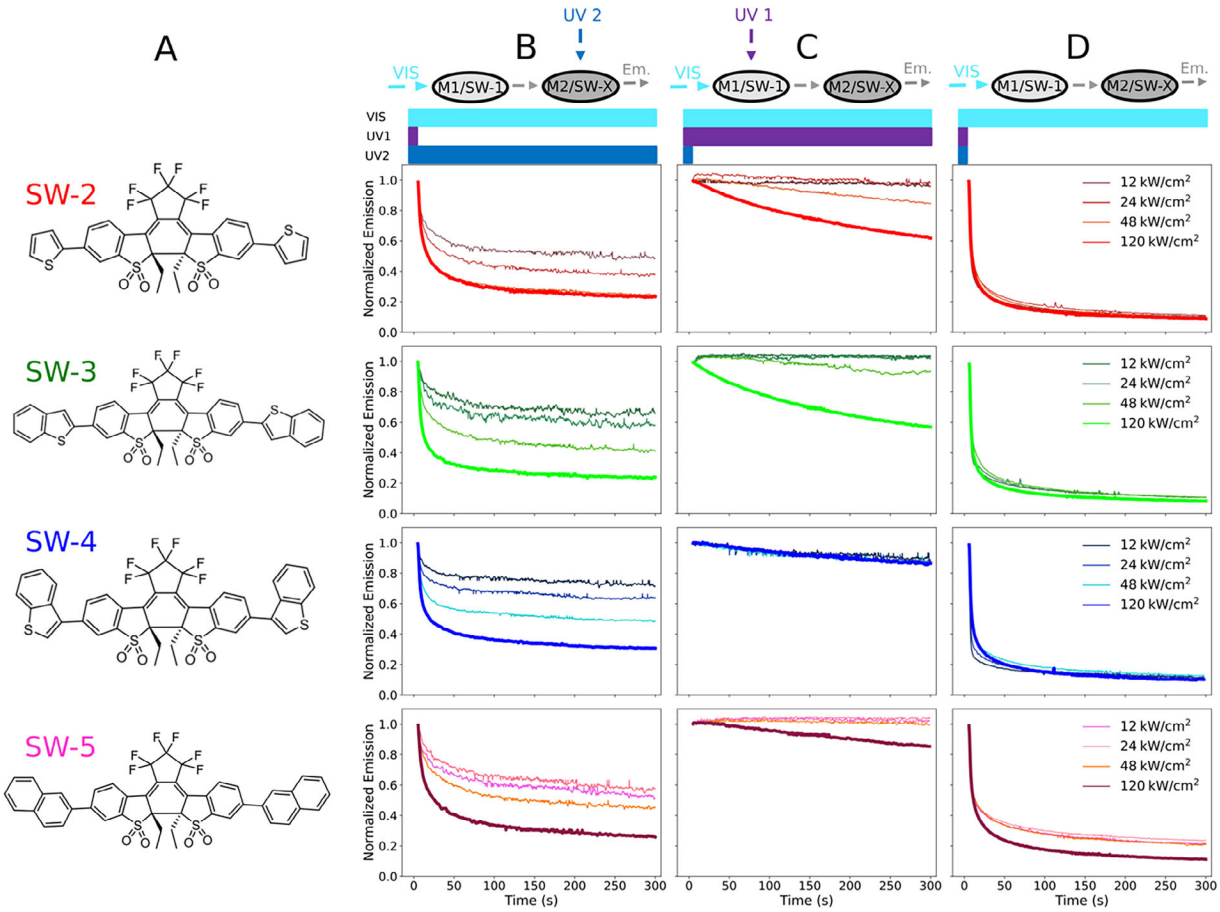

Figure 7. Emission intensities from SW-X molecules on M2 and SW-1 molecules on M1 for three different illumination scenarios, and four different VIS intensities. The columns show, from left to right, the molecular structure the photochromic molecules used on M2, and the relative decrease of the emission from the sample on M2 for the three illumination scenarios. For each scenario, the experiments have been conducted for fixed excitation intensities of 28 W cm^{-2} for UV1 and 0.8 W cm^{-2} for UV2, and four different excitation intensities for the VIS radiation as given in the figure. The traces have been normalized to the data point at $t = 5\,s + 200\,ms$, which corresponds to the first data point after the UV1 (part B), UV2 (part C), or UV1 and UV2 (part D) illuminations were ceased. The traces for the illumination conditions that gave the highest contrast are highlighted as bold lines. The maximum contrasts that have been read out for $I_{max} = I(5s + 200\,ms)$ and $I_{min} = I(300\,s)$ are summarized in Table 1.

from SW-1, because more and more SW-1 molecules are converted to the LE state under the continuous illumination with the VIS laser, which reduces the intensity available for exciting SW-3 in the visible. Second, the visible radiation that is still absorbed by SW-3 can also induce the cycloreversion process of the SW-3 molecules and convert them to the LE state, which further diminishes the emission intensity from SW-3. Hence, the fast decay of the emission of SW-3 in Figure 6C is the result of two processes that enhance each other.

Similar experiments as shown in Figure 6 have also been conducted for the other photochromic molecules SW-X on M2. The results obtained for these combinations of photoswitches are

Table 1. Maximum achieved values of the contrast for the emission intensity of SW-X (X = 2, 3, 4, or 5) upon excitation via SW-1.

	UV 2 / VIS / M1/SW-1 / M2/SW-X / Em.	UV 1 / VIS / M1/SW-1 / M2/SW-X / Em.	VIS / M1/SW-1 / M2/SW-X / Em.
VIS intensity [kW cm^{-2}]	120	120	120
		Contrast	
SW-2	0.77	0.38	0.91
SW-3	0.76	0.43	0.92
SW-4	0.68	0.14	0.90
SW-5	0.76	0.15	0.89

Table 2. The truth table for the experiment is sketched in Figure 7, where the presence and absence of UV1 and UV2 serve as Boolean input variables, and the fluorescence from SW-X as output variable.

In		Out
HE-SW-1	HE-SW-X	High emission
0	0	0
0	1	0
1	0	0
1	1	1

summarized in **Figure 7**. The figure has the layout of a matrix where each line corresponds to one particular photochromic molecule on M2, the first column of the figure refers to the chemical structure of the photochromic molecules in the closed state (HE state), and the last three columns correspond to the signals obtained for the three excitation scenarios as shown in Figure 6, and indicated by the symbols at the top of Figure 7, each one for four different intensities of the VIS laser incident on M1. The achievable contrasts show strong variations as a function of the VIS intensity, and their maximum values are summarized in **Table 1**.

For all of the photochromic molecules used on M2 and for all three illumination scenarios we find a constant and high emission intensity from SW-X only during the interval where both UV sources are ON, see Figure 7. As soon as one of the UV sources is switched OFF the emission from SW-X drops rapidly to a lower level. Hence, the UV photons that were required to create the HE states of the photochromic molecules both on M1 and M2 were translated into fluorescence photons from the photochromic molecules on M2. Interpreting the creation of a photochromic molecule in the HE state and LE state as logic inputs 1 and 0, and defining the emission levels of SW-X as logical 1 (initial high emission) and 0 (decreasing emission), the outcome of the experiment can be summarized in **Table 2**. Closer inspection reveals that this table can be identified with the truth table for an (optical) AND gate. This demonstrates that the translation of UV photons into fluorescence photons mediated by photochromic molecules fulfills the rules of boolean algebra for an AND gate, accomplished solely by optical inputs and outputs.

4. Conclusion

In a proof-of-principle experiment, the realization of an all-optical AND gate in the solid state has been demonstrated. This was achieved using photochromic DAE derivatives as mediators for the optical input signals. These molecules are photostable and fatigue-resistant and it will be challenging to extend this approach to more complex operations (OR, NOR, XOR, etc. operations), that will be required to accomplish full optical logic circuits. Further challenges that need to be addressed are the seamless integration and miniaturization of the components as well as a reduction of the reaction times for signal processing.

Supporting Information

Supporting Information is available from the Wiley Online Library or from the author.

Acknowledgements

J.K. and M.T. thankfully acknowledge financial support by the Deutsche Forschungsgemeinschaft (Ko 1359/30-1, TH 807/11-1, GRK 2818) and the Bavarian State Ministry for Arts and Science within the initiative "Solar Technologies go Hybrid". P.M. thanks the ARC Centre of Excellence in Exciton Science for support through CE170100026.

Open access funding enabled and organized by Projekt DEAL.

Conflict of Interest

The authors declare no conflict of interest.

Data Availability Statement

The data that support the findings of this study are available from the corresponding author upon reasonable request.

Keywords

photochromic molecules, photonic logic gates, semiconductor quantum

Received: March 20, 2025
Revised: May 2, 2025
Published online:

[1] M. Irie, *Chem. Rev.* **2000**, *100*, 1685.
[2] M. Irie, T. Fukaminato, K. Matsuda, S. Kobatake, *Chem. Rev.* **2014**, *114*, 12174.
[3] J. Andréasson, U. Pischel, *Coordin. Chem. Rev.* **2021**, *429*, 213695.
[4] T. Fukaminato, S. Ishida, R. Metivier, *NPG Asia Mater.* **2018**, *10*, 859.
[5] S. Kobatake, S. Takami, H. Muto, T. Ishikawa, M. Irie, *Nature* **2007**, *446*, 778.
[6] W. A. Velema, W. Szymanski, B. L. Feringa, *J. Am. Chem. Soc.* **2014**, *136*, 2178.
[7] B. Roubinet, M. L. Bossi, P. Alt, M. Leutenegger, H. Shojaei, S. Schnorrenberg, S. Nizamov, M. Irie, V. N. Belov, S. W. Hell, *Angew. Chem., Int. Ed.* **2016**, *55*, 15429.
[8] M. Pärs, K. Gräf, P. Bauer, M. Thelakkat, J. Köhler, *Appl. Phys. Lett.* **2013**, *103*, 221115.
[9] M. Pärs, C. C. Hofmann, K. Willinger, P. Bauer, M. Thelakkat, J. Köhler, *Angew. Chem., Int. Ed.* **2011**, *50*, 11405.
[10] O. Nevskyi, D. Sysoiev, A. Oppermann, T. Huhn, D. Wöll, *Angew. Chem., Int. Ed.* **2016**, *55*, 12698.
[11] M. Barale, M. Escadeillas, G. Taupier, Y. Molard, C. Orione, E. Caytan, R. Métivier, J. Boixel, *J. Phys. Chem. Lett.* **2022**, *13*, 10936.
[12] B. Daly, T. S. Moody, A. J. M. Huxley, C. Yao, B. Schazmann, A. Alves-Areias, J. F. Malone, H. Q. N. Gunaratne, P. Nockemann, A. P. de Silva, *Nat. Commun.* **2019**, *10*, 49.
[13] O. Nevskyi, D. Sysoiev, J. Dreier, S. C. Stein, A. Oppermann, F. Lemken, T. Janke, J. Enderlein, I. Testa, T. Huhn, D. Wöll, *Small* **2018**, *14*, 1703333.
[14] U. Pischel, J. Andréasson, D. Gust, V. F. Pais, *ChemPhysChem* **2013**, *14*, 28.
[15] M. Berberich, A.-M. Krause, M. Orlandi, F. Scandola, F. Würthner, *Angew. Chem., Int. Ed.* **2008**, *47*, 6616.
[16] G. Berkovic, V. Krongauz, V. Weiss, *Chem. Rev.* **2000**, *100*, 1741.
[17] J. Andreasson, S. D. Straight, T. A. Moore, A. L. Moore, D. Gust, *Chemistry* **2009**, *15*, 3936.
[18] J. Andreasson, U. Pischel, *Chem. Soc. Rev.* **2018**, *47*, 2266.

[19] H. Zhang, P. Dharpure, M. Philipp, P. Mulvaney, M. Thelakkat, J. Köhler, *Adv. Opt. Mater.* **2024**, *12*, 2401029.
[20] S. Zanella, M. A. Hernández-Rodríguez, L. Fu, R. Shi, L. D. Carlos, R. A. S. Ferreira, C. D. S. Brites, *Adv. Opt. Mater.* **2023**, *20*, 327.
[21] S. Zanella, M. A. Hernández-Rodríguez, R. A. S. Ferreira, C. D. S. Brites, *Chem. Commun.* **2023**, *59*, 7863.
[22] Y.-C. Jeong, S. I. Yang, K.-H. Ahn, E. Kim, *Chem. Commun.* **2005**, *19*, 2503.
[23] K. Uno, H. Niikura, M. Morimoto, Y. Ishibashi, H. Miyasaka, M. Irie, *J. Am. Chem. Soc.* **2011**, *133*, 13558.
[24] A. Albert, M. Fried, M. Thelakkat, J. Köhler, *Phys. Chem. Chem. Phys.* **2022**, *24*, 29791.